Journal of Aerosol Science 73 (2014) 48–62

Contents lists available at ScienceDirect

Journal of Aerosol Science

journal homepage: www.elsevier.com/locate/jaerosci

Measuring particulate matter emissions during parked active diesel particulate filter regeneration of heavy-duty diesel trucks

David C. Quiros [a,b,*], Seungju Yoon [c], Harry A. Dwyer [d], John F. Collins [c], Yifang Zhu [e], Tao Huai [a]

[a] Monitoring and Laboratory Division, California Air Resources Board, 1900 14th Street, Sacramento, CA 95811, USA
[b] Environmental Science & Engineering, Institute of the Environment and Sustainability, University of California, Los Angeles, La Kretz Hall, Suite 300, Los Angeles, CA 90095-1496, USA
[c] Research Division, California Air Resources Board, 1001 I Street, Sacramento, CA 95814, USA
[d] Department of Mechanical and Aerospace Engineering, University of California, Davis 2131 Bainer Hall, Davis, CA 95616, USA
[e] Environmental Health Sciences, Fielding School of Public Health, University of California, Los Angeles, 650 Charles E. Young Drive South, Los Angeles, CA 90095, USA

ARTICLE INFO

Article history:
Received 30 December 2013
Received in revised form
12 March 2014
Accepted 15 March 2014
Available online 24 March 2014

Keywords:
Diesel particulate filter
Regeneration
Particulate matter
Effective density
Ambient dilution

ABSTRACT

Heavy-duty diesel trucks (HDDTs, $>33{,}000$ pounds gross vehicle weight rating) are commonly equipped with diesel particulate filters (DPFs) to meet the California model year (MY) 2007 PM emissions standard. Particulate matter (PM) emissions were measured from nine parked active DPF regenerations of two HDDTs, a 2007 and 2010 MY, using a novel ambient-dilution wind tunnel. This work specifically evaluated PM mass emissions during regeneration by measurements from the following instruments: TSI DustTrak DRX 8533, TSI Engine Exhaust Particle Sizer 3090 (EEPS) and TSI Scanning Mobility Particle Sizer 3936L88 (SMPS), filters by gravimetric analysis, and for one test a Dekati Mass Monitor 230-A (DMM). Active regeneration by fuel injection upstream of the DPF began with the Soot Combustion Regime, where PM emissions had a count median diameter (CMD) of >30 nm and some faint gray smoke was observed flowing from the tunnel. During brief moments of the Soot Combustion Regime, the DustTrak DRX reported more than half of the mass was >1 μm. As active regeneration continued, aftertreatment inlet temperature increased to >500 °C, beginning the Fuel Combustion Regime, defined conversely where the CMD of the emissions was <30 nm. Under both regimes, discrepancies were observed between EEPS and SMPS size distributions and improved agreement was attained after performing a post-hoc EEPS correction procedure. The accuracy of the DMM was equivocal; the average DMM emissions rate was within five percent of the gravimetric filter, but the mass distribution was substantially shifted relative to SMPS and EEPS distributions. Uninterrupted parked active regeneration resulted in 13 g PM emissions from the 2007 MY and 1.8 g PM from the 2010 MY based on filter measurements. The PM mass emissions rates, based on measurements from real-time instruments, show that the contribution of Soot Combustion Regime to total regeneration emissions decreased from 75% to 5% between the 2007 and 2010 MY.

* Corresponding author at: Monitoring and Laboratory Division, California Air Resources Board, 1900 14th Street, Sacramento, CA 95811, USA. Tel.: +1 916 445 9370; fax: +1 916 324 1556.
E-mail address: dquiros@arb.ca.gov (D.C. Quiros).

http://dx.doi.org/10.1016/j.jaerosci.2014.03.002
0021-8502/

1. Introduction

Diesel particulate matter (PM) emissions from mobile sources are a key regulatory priority for the California Air Resources Board (CARB) and the United States Environmental Protection Agency (U.S. EPA) (US) (EPA, 2002; Lloyd & Cackette, 2001). The PM emission standard for a 2007 model year (MY) or later heavy-duty diesel truck (HDDT, $>33{,}000$ pounds gross vehicle weight rating) is 0.01 g/bhp-h; other regulated pollutants include carbon monoxide 15.5 g/bhp-h, non-methane hydrocarbons 0.14 g/bhp-h, and nitrogen oxides 0.20 g/bhp-h (nitrogen oxide standard was not required until 2010). Engine operation modifications and exhaust aftertreatment devices such as the diesel particulate filter (DPF) and selective catalytic reduction (SCR) are key approaches to meet these stringent standards.

Periodically, DPFs must be regenerated to remove accumulated particulates such as soot and organic materials. Regeneration is initiated either actively by fuel injection upstream of the DPF or passively during aggressive engine duty cycles generating high exhaust temperatures. During regeneration, large quantities of PM are emitted, mostly as semi-volatile or sulfate materials (Barone et al., 2010; Cauda et al., 2007; Herner et al., 2011; Khalek et al., 2011; Kittelson et al., 2006). However, the scientific community has not reached consensus on the most appropriate sampling method for new-technology vehicle emissions (Khalek et al., 2011; May et al., 2013).

Real-time PM instrumentation has been successfully applied to vehicle emission studies measuring passive DPF regeneration. For example, Khan et al. (2012) compared various portable emissions measurement systems (PEMS) and showed strong correlation ($R^2=0.78$) between the Dekati Mass Monitor (DMM, 0–1.3 μm) and gravimetric measurements from a calibrated 1065-compliant mobile emissions laboratory. Another successful study, Z.G. Liu et al. (2009), measured particle size distribution (PSD) using the TSI Engine Exhaust Particle Sizer (EEPS, 5.6–560 nm) and applied an effective density function from Maricq & Xu (2004) to calculate PM mass. However to the best of our knowledge, PM emissions have not been reported during parked active DPF regeneration where no useful work is produced by the engine. Many HDDTs persistently operate at light engine loads (e.g. inner-city buses and drayage trucks), do not initiate passive DPF regeneration, and therefore a parked active regeneration is conducted to remove accumulated PM deposits. Furthermore, many in-use HDDTs used for long-haul operation also may require an occasional parked active DPF regeneration. Therefore, the PM emissions during parked active DPF regeneration are expected to be observed from a variety of HDDT applications.

This study presents PM emissions during parked active DPF regenerations of a 2007 and 2010 MY HDDT measured using a novel ambient-dilution wind tunnel. The broad objective of this study is to evaluate PM emissions explicitly during regeneration without any applied engine load under controlled conditions using ambient air. The present objective is to evaluate the performance of the following PM instrumentation when challenged with ambient-diluted regeneration emissions: TSI DustTrak DRX 8533, TSI Engine Exhaust Particle Sizer (EEPS, 3090), TSI Scanning Mobility Particle Sizer (SMPS, 3936L88), and Teflon-coated borosilicate filters with gravimetric analysis. For one regeneration, a Dekati Mass Monitor 230-A was included for direct mass measurements. This work classifies parked active DPF regeneration emissions into two distinct regimes defined by count median diameter (CMD) of the distribution. The characteristics, merits, and limitations of each real-time instrument are discussed.

2. Materials and methods

2.1. Facility

Experimental work was conducted at the California Air Resources Board (CARB) Depot Park Facility located approximately 10 km southeast of downtown Sacramento, CA. Within the Depot Park Facility boundaries, there are several small private roads with sparse traffic and combustion sources. The impacts of transient local source emissions on test results were assumed negligible because no sudden increases in particle number concentration were observed during ambient monitoring and the study location was located greater than 500 m from the nearest public roadway (Zhu et al., 2002). We assume the ambient dilution air was stable over the measurement period and represents a typical urban or suburban background. Although the contribution to measurements is quantified, we did not apply any background correction for our measurements.

2.2. Testing vehicles and setup

Two Kenworth HDDTs were tested in this study; one was outfitted with a 2007 Cummins engine with a diesel oxidation catalyst (DOC) and a DPF (2007 MY), and another a 2010 Cummins engine with a DOC, DPF, and SCR aftertreatment system (2010 MY). Commercial-grade ultralow sulfur diesel fuel (<15 ppm sulfur) was used during the testing of these vehicles. Prior to the study, the odometers read 391,000 miles and 18,600 miles for the 2007 and 2010 HDDTs, respectively. Aftertreatment equipment was neither replaced nor ash cleaned within one year of this study.

Figure 1 illustrates the routing of exhaust gases into the ambient-dilution wind tunnel. A circular steel deflection plate was affixed 50 cm downstream of and perpendicular to the exhaust transfer tube to induce rapid mixing. Temperature measurements on horizontal and vertical traverses were made at various distances from initial mixing to ensure the mixture of exhaust gases and ambient air was homogenous at the sampling location (Dwyer, 2013). The ambient-dilution wind tunnel flow used during this study of 9000 ft^3/min (CFM) resulted in a residence time of 7.2 s. A sampling probe facing

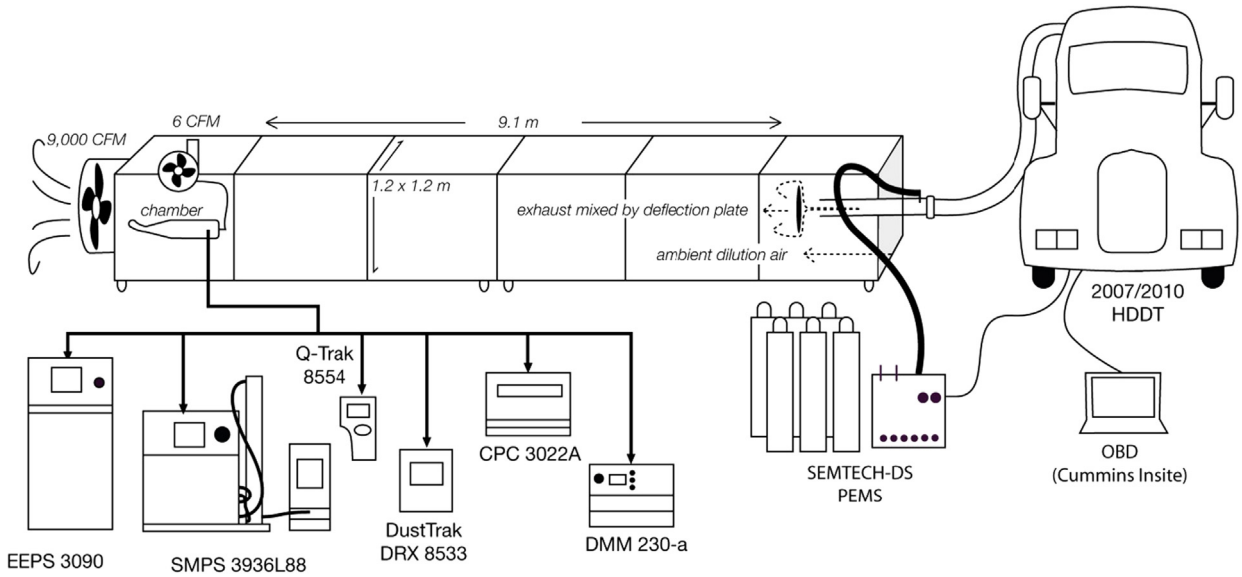

Fig. 1. Setup of the parked HDDT, ambient-dilution wind tunnel, and instrumentation.

Table 1
Instruments measuring raw exhaust, Tunnel Emissions (Chamber), and to obtain information from the on-board diagnostic (OBD) system.

Device	Parameter	Detection limits	Op. temp (°C)	Location
SEMTECH-DS	CO_2, exhaust flow	0–200,000 ppm, N/A	0–45	Raw exhaust
Cummins INSITE	DPF loading	N/A	N/A	OBD
TSI SMPS 3936L88	PSD (5.4–198 nm)	2×10^7 #/cm^3	10–35	Chamber
TSI EEPS 3090	PSD (5.6–560 nm)	5.6 nm: 10^8 #/cm^3 560 nm: 10^6 #/cm^3	0–40	Chamber
TSI CPC 3022A	PNC (7 nm–3 μm)	10^7 #/cm^3	0–35	Chamber
TSI DustTrak DRX 8533	PM_1, $PM_{2.5}$, PM_{10}	>0.1 μm: 0.001–150 mg/m^3	0–50	Chamber
TSI Q-Trak 8554	CO_2	0–5000 ppm	0–50	Chamber
Dekati Mass Monitor 230-a	Mass 0.01–1.3 μm	1–5000 μg/m^3	5–40	Chamber
Teflon-coated filters	Mass	1-μg resolution	Ambient	Chamber

upstream at the centerline of the ambient-dilution tunnel drew 6 CFM into a sample chamber. The sampling chamber intake was superisokinetic where tunnel flow was 2.85 m/s and chamber intake flow was 1.40 m/s. Sampling probe intake from the chamber ranged from subisokinetic to superisokinetic where chamber flow was 22 cm/s and upstream-facing probe intake velocities ranged 15–210 cm/s. Although aerosol sampling occurred under a range of anisokinetic conditions, the Stokes number was less than 10^{-3} for a 10-μm particle of unit density, indicating negligible impact on the sampling of the particle sizes observed during this study (Hinds, 1999). During regeneration periods, exhaust flow was 290 and 250 CFM, and dilution ratio was 31 and 36 for the 2007 and 2010 MY, respectively. The greater dilution ratio of 36 for the 2010 MY compared to the ratio of 31 for the 2007 MY may have, to some degree, impacted the PM size distribution or concentration. However, the difference in dilution ratio is expected to have a smaller effect than the difference of emissions between the two engines. A constant tunnel flow rate of 9000 CFM was used for this study; evaluation of tunnel flow rate and therefore residence time and dilution ratio, is beyond the scope of this work.

2.3. Instrumentation

The instrumentation in the study is described in detail in Table 1. On-board diagnostic (OBD) data were obtained from Insite Lite 7.5.0.234 (Cummins Inc., Columbus, IN, USA); this tool also enabled the "forced" parked active DPF regeneration when not otherwise permitted by the dashboard control. A PEMS, the SEMTECH-DS (Sensors, Inc., Saline, MI, USA) was used to measure CO_2 concentration and exhaust flow, which were used calculate dilution ratio based on total tunnel flow and mixed exhaust CO_2 measured from a TSI Q-Trak 8554. The Q-Trak also reported temperature and relative humidity of mixed exhaust. The real-time PM instrumentation included the TSI Engine Exhaust Particle Sizer 3090 (EEPS, TSI incorporated,

Shoreview, MN, USA), TSI Scanning Mobility Particle Sizer 3936L88 (SMPS), TSI DustTrak DRX 8533 (DustTrak), and Dekati Mass Monitor 230-a (DMM, Kangasala, Finland).

2.3.1. Filter gravimetric analysis

Gravimetric filter media were 47-mm Pallflex Fiberfilm T60A20 (polytetrafluoroethylene-coated borosilicate glass fibers) manufactured by Pall (Port Washington, NY, USA). Sampling flow rate was 6 CFM, corresponding to an approximate filter-face velocity of 164 cm/s, and sample media was maintained at ambient-dilution exhaust temperatures ranging 18–38 °C. Comparability to 40 CFR 1065 compliant PM measurements is unclear due to larger filter-face velocities and the absence of any temperature control in this study. However, Bushkuhl et al. (2013) found gas-particle partitioning of measured PM within the limited temperature range and equilibrium was not discerned from test variability. PM collection onto filters commenced before the first ambient measurement lasting until the end of the second ambient measurement; no independent ambient sample was collected. Sampling flows for filters and real-time instruments were drawn from the same sampling chamber manifold so that measurements were collected under identical dilution ratio and temperature conditions.

2.3.2. EEPS

The TSI EEPS 3090 measured a 32-channel PSD from 5.6 to 560 nm by classifying positive corona charged particles according to electrical mobility. The EEPS was developed by Johnson et al. (2004), and has been used for laboratory (e.g. J. Wang et al., 2006) and on-road (e.g. Kittelson et al., 2006) engine exhaust sampling studies because of its fast 10-Hz sampling resolution. However because unipolar charge accumulation may be greater for a particle of lower fractal dimension than of its mobility diameter equivalent sphere (Asbach et al., 2009; Oh et al., 2004), particle morphology can bias the size classification and reported size concentration. The accuracy of an EEPS-reported size distribution would be bolstered by quality assurance and quality control procedures. For this study, SMPS measurements were also collected (Section 2.3.3).

The detection column was cleaned following the basic procedure described in the manual twice during this study. This process involves using an acrylic cylinder and lint-free cloth to remove deposited PM from the electrode rings, followed by a zeroing of the electrical current readings. The zeroing procedure was performed a few additional times during the study; electrometer offsets were typically less than 15 fA, electrometer noise values (RMS) were less than 10 fA, and both were stable between successive zeroing procedures. The auxiliary column heater option was not used. Data collection was conducted using the TSI EEPS software release version 3.1.1.0 and the instrument was running firmware version MCU 3.04 DSP 3.01.

2.3.3. SMPS

The TSI SMPS 3936L88 measured a 100-channel PSD from 5.5 to 198 nm by classifying a bipolar charged distribution according to electrical mobility. Aerosol is neutralized to Boltzmann equilibrium, classified by a Differential Mobility Analyzer (DMA) with continuously varying voltage (S.C. Wang & Flagan, 1990) on a two-minute time resolution. Particles are detected with a condensation particle counter (CPC) to produce a PSD using a software tool accounting for transfer functions and transport-time delays (Russell et al., 1995).

The TSI SMPS 3936L88 used for this study employed an Electrostatic Classifier (EC 3080), with a Long DMA 3081, and a Nano-Water-Based Condensation Particle Counter (N-WCPC 3788). A 0.071-cm inlet impactor was used to remove particles of larger aerodynamic diameter capable of carrying multiple charges that could be mistakenly classified within the measurement range. The EC sheath flow rate was 18 L/min and N-WCPC aerosol flow rate was 0.6 L/min thereby achieving a sheath-to-aerosol flow ratio of 30 and a narrow transfer function between 5.5 and 198 nm. The TSI Aerosol Instrument Manager (AIM) Software Version was 9.0.0, using Diffusion Correction to correct for internal instrument losses and Multiple Charge Correction to attain an accurate size distribution within the electrical mobility range based on a typical Boltzmann charge distribution. Nanoparticle Aggregate Mobility Analysis was not used because we did not expect dry fractal agglomerates and did not measure primary particle size.

2.3.4. DustTrak DRX

The TSI DustTrak DRX 8533 combines photometric measurement for measuring fine particles ($PM_{2.5}$) with laser-based single particle sizing for reporting additional size fractions (PM_1, PM_4, PM_{10}, and PM_{Total}). The total mass concentration is estimated by combining the signal from the 655-nm wavelength photometer and single particle laser pulse height signals. The result of using a dual-measurement approach is a fractionated and more sensitive PM mass measurement than previous DustTrak models, and measurement over a wider concentration range (X. Wang et al., 2009). The instrument does not measure PM mass from ultrafine particles (UFPs, < 100 nm) as they are undetected by the photometer. Consistent with calibration of previous DustTrak models, factory calibration is based on the density, refractive index, and shape factor of Arizona Test Dust (ATD, ISO 12103-1, A1). This work seeks to establish new relationships between the ATD calibration and ambient-diluted exhaust, similar to the calibration factor of 1/2.4 established by Yanosky et al. (2002) that is widely used in other vehicle emissions studies.

2.3.5. DMM

The DMM 230-A applies a positive corona charge to an influent aerosol stream, which is first classified by an electrical mobility channel followed by inertial impaction (Lehmann et al., 2004). The ratio of mobility and aerodynamic lognormal distributions is calculated for the mobility region (10–30 nm), and extended to larger sizes by applying a decreasing density function observed with increasing size for dry fractal soot agglomerates defined by Virtanen et al. (2002). When the majority of the total aerosol charge is detected by the mobility region, the instrument assumes a dominant nucleation mode and applies 1 g/cm^3 for all particle sizes. These procedures for measuring and applying density are both repeated at 1 Hz. Accordingly, the DMM is designed to accurately measure low and high PM mass concentrations for a wide range of particle sizes, and has been tested over the past decade in comparison to the traditional gravimetric method (Khalek, 2005; Khan et al., 2012; Mamakos et al., 2006). Data were collected using PC software version 1.2 rev 202, and daily cleaning and quality assurance procedures were followed according to the manual. The DMM was used in the present study only for test 3-A, the third Initial Regeneration event of the 2007 HDDT.

2.4. Procedure: Initial and Subsequent Regenerations

Before performing DPF regeneration, each HDDT was driven at low roadway speeds for up to thirty hours to accumulate material onto inner DPF surfaces without inducing a passive regeneration event. The parked active regenerations performed in this study were classified into two groups: Initial Regenerations and Subsequent Regenerations. Table 2 shows the five Initial Regenerations in this study (test IDs ending with "A"), which were performed on fully loaded DPFs. Initial Regenerations 1-A and 3-A were performed on higher levels of DPF loading than events 2-A, 4-A, and 5-A, which was indicated by a flashing dashboard indicator light and a data channel from the Insite OBD Tool. Four Subsequent Regenerations were measured (IDs ending with a "B, C, or D,"), which were initiated after the previous regeneration without any additional DPF loading.

All regeneration events followed the same protocol including the following order of measurements: ambient with engine off (ambient, 10 min), curb idle (idle, 10 min), regeneration (10–40 min), idle (10 min), ambient (10 min). Under this experimental design, measurements reflect the total mass flux of PM from ambient dilution air and from engine exhaust. The total Tunnel Emissions rate (g PM/h) is reported for each phase of the test sequence rather than subtracting the ambient from total mass flux. This approach facilitates a simple evaluation of ambient-diluted engine emissions between phases. Unless indicated, the contribution of PM from ambient dilution air was a negligible fraction of the Tunnel Emissions rate.

2.5. Analyses

2.5.1. Tunnel and sampling line losses

To minimize electrostatic sampling losses, conductive silicon tubing was used for all instruments except for the DMM where Tygon tubing was used per manufacturer specification (B.Y.H. Liu et al., 1985; Timko et al., 2009). Measurements for all instruments were corrected for diffusional losses by multiplying measured particle number by the inverse of penetration, μ, defined below in Eq. (1) (Hinds, 1999):

$$\mu = D \times L \times Q^{-1} \tag{1}$$

where D is the diffusion coefficient of the particles, L is the length of the tube, and Q is the volume flow through the sampling line. Because diffusional coefficient D is a function of particle size, SMPS and EEPS data were corrected individually by size channel, and DustTrak and DMM data were corrected individually at 1 Hz based on the CMD value of the EEPS distribution. Although actual corrections varied throughout the testing depending on the size distribution, the following approximate corrections were made for each instrument if all particles were 20 nm: 7% (SMPS), 2.1% (DustTrak), 1.3%

Table 2
Description of DPF regeneration and characteristics of ambient dilution air for each test. Each parameter was measured for ten minutes before and after testing; reported are the averages of the two periods as measured by the Q-Trak for temperature and relative humidity (RH), and DustTrak DRX for $PM_{2.5}$.

ID	Truck	DPF loading state	Classification	Shutoff method	Duration [s]	Ambient parameters		
						Temp [°C]	RH [%]	$PM_{2.5}$ [μg/m^3]
1-A	2007	Above Normal – Severe	Initial	Manual abort	881	14.6	37.0	7.66
1-B	2007	Above Normal – Least Severe	Subsequent	Manual abort	955	15.4	34.3	3.62
1-C	2007	Above Normal – Least Severe	Subsequent	Automatic	1200	11.3	49.9	32.4
1-D[a]	2007	Normal	Subsequent	Automatic	2411	14.4	36.1	41.2
2-A	2007	Above Normal – Least Severe	Initial	Automatic	1512	12.5	63.5	13.0
3-A	2007	Above Normal – Severe	Initial	Automatic	2415	34.0	9.7	4.21
4-A	2010	Above Normal – Least Severe	Initial	Automatic	2730	15.1	56.0	26.2
4-B[a]	2010	Normal	Subsequent	Automatic	1335	22.6	40.8	26.9
5-A	2010	Above Normal – Least Severe	Initial	Automatic	1000	19.8	17.7	9.33

[a] Forced parked active regeneration, initiated by on-board diagnostic (OBD) Insite Lite 7.5.0.234 tool.

(DMM), and 0.9% (EEPS). The calculated penetration of a 20-nm particle from the point of exhaust mixing with ambient air to the instrument-level sampling ports was greater than 99.7% (Hinds, 1999). Therefore, particle losses to the inner walls of the ambient-dilution tunnel were negligible, and no correction was applied.

2.5.2. EEPS zero correction (C_1)

The upper detection limit of the EEPS (10^8/cm^3 at 5.6 nm, 10^6/cm^3 at 560 nm) was often approached during regeneration events due to high PM emissions. When measuring near the upper detection limit, the TSI EEPS software reported zero particle counts for some groups of channels that we expected to be non-zero positive values. The zeroes were observed similarly before and after EEPS electrometer cleaning, zeroing, and replacing corona charging needles, but not in PSD measured by the SMPS. A similar pattern is shown by Zheng et al. (2011) where channels of the EEPS distribution are zero adjacent to the peak also when measuring HDDT emissions. The cause of this phenomenon could be condensation of hygroscopic sulfates during these high-particle events that may have been prevented by using the column heater option (TSI, 2011), or that the data inversion algorithm may have not properly accounted for irregularities when electrometers approached detection limits. Data in this study were corrected by linear and power-function regression analyses that are described in more detail in Section 1 of Supporting information. Data corrected using this procedure are appended as EEPS (C_1). The corrected distribution is still an underestimate of actual concentrations when the detection limit is exceeded for the maximized channels. We recommend future studies employ higher primary or secondary dilution to attain a total dilution ratio of at least 100 when measuring emissions during parked active DPF regeneration.

2.5.3. Calculating PM mass from EEPS and SMPS

The EEPS and SMPS report PSD as the derivative of particle number with respect to size, $dN/d\log D_m$. The distribution of the derivative is converted to the spherical mobility-equivalent volume ($dV/d\log D_m$). PM mass is calculated by multiplying $dV/d\log D_m$ and a particle effective density function defined in Eq. (2) (Z.G. Liu et al., 2009; Maricq and Xu, 2004), where D_m is electrical mobility diameter:

$$\rho_{effective} = 1.2378 \times \exp(-0.0048 \times D_m) \quad (2)$$

This exponential decay function was applied for all particles and decays sharply 1.20 g/cm^3 for a 5.6-nm particle to 0.08 g/cm^3 for a 560-nm particle. This density was derived from both emissions of both direct-injection gasoline and diesel vehicles, and has been successfully applied to heavy-duty diesel engine emissions. Although the accuracy for active DPF regeneration emissions is unknown, the function is a valid reference that can be used to precisely measure PM mass.

3. Results and discussion

3.1. 2007 MY HDDT

3.1.1. Two Regeneration regimes

Figure 2 shows a contour plot of the size distribution emitted during test 3-A, an Initial Regeneration of the 2007 HDDT. Within the first 500 s of regeneration (1200–1700 s of the test sequence), some faint gray smoke was observed leaving the tunnel, and the CMD of the distribution was between 100 and 200 nm. This may be due to oxidation of material from accumulated PM on inner DPF surfaces that reached their minimum activation energy (Burtscher, 2005; Maricq, 2007) as aftertreatment temperatures increased gradually and plateaued at temperatures above 500 °C. Under this paradigm, materials emitted between 1300 and 1500 s of the test sequence were more volatile and abundant than those released later between 1500 and 1700 s of the test sequence. However, the material accumulated upon filter media was faint yellow;

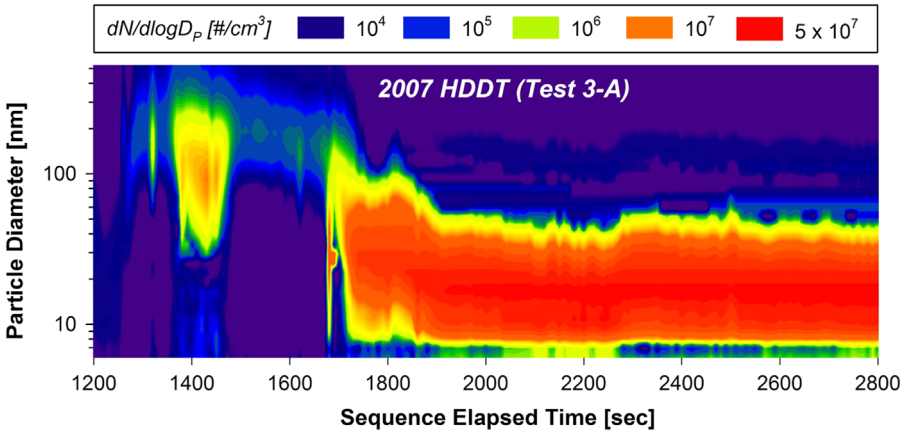

Fig. 2. Contour plot showing EEPS (C_1) number-based size distributions during test 3-A, an Initial Regeneration of the 2007 HDDT.

alternatively some of the emissions between 1200 and 1700 s could have been condensed engine oil downstream of the DPF. Although the composition remains unknown, this phase will hereafter referred to as the "Soot Combustion Regime", defined as whenever the CMD is >30 nm during regeneration. Test 3-A was selected for discussion because it was uninterrupted from start to finish and the initial DPF loading was the greatest of the tests in the study. During this test, the Soot Combustion Regime accounted for 75% of the PM mass emissions of the parked regeneration based on an empirical combination of the real-time measurements. The remaining 25% of PM mass emissions were emitted after the Soot Combustion Regime.

Figure 2 shows that as active regeneration by fuel injection continued during test 3-A, CMD stabilized near 20 nm beginning around 1700 s of the test sequence. The CMD and GSD remained essentially unchanged for the remainder of the Initial Regeneration. Therefore for simplicity, whenever the CMD of the size distribution was <30 nm, the DPF regeneration stage was defined as the "Fuel Combustion Regime." These emissions may have been due to the high-temperature catalytic conversion of SO_2 to SO_3 documented during DPF regeneration when applying engine load (Grose et al., 2006; Herner et al., 2011). However, the regeneration emissions with a CMD between 15 and 25 nm contrasts with emissions where CMD was <10 nm observed during slow and gradual passive regeneration due to engine-generated heat (Herner et al., 2011).

3.1.2. Real-time PM mass emissions

Figure 3 presents the mass flux through the ambient-dilution tunnel (hereafter: Tunnel Emissions, g PM/h) from test ID 3-A measured by the EEPS (C_1, 5.6–560 nm), SMPS (5.4–198 nm), DustTrak PM_{10} and PM_1, and DMM (0.01–1.3 μm). Tunnel Emissions for all instruments remained unchanged from ambient to idle after engine cold-start (600 s) and from idle to ambient after turning the engine off (4200 s). The response of the instruments to the Soot and Fuel Combustion Regimes were dramatic and are described by each instrument in the following subsections.

3.1.2.1. DustTrak DRX. Within the Soot Combustion Regime, Fig. 3 shows that DustTrak PM_{10} and PM_1 Tunnel Emissions peaked at 630 g and 480 g PM/h and are much larger than measured by all other instruments. DustTrak size fractions are shown more clearly in Fig. 4(a) where tunnel concentration is reported on a linear scale. At around 1280 s, tunnel PM was apparently ~40% larger than 1 μm, which is surprising because mechanical or extended atmospheric processing is typically required for generating PM in the fine and coarse size ranges (Harrison et al., 2000). This distribution with large particle sizes was only observed for regeneration events 1-A and 3-A where DPF loading was "Above Normal – Severe". Figure 4(b) shows all tunnel PM was smaller than 1 μm during test ID 2-A when DPF loading was "Above Normal – Least Severe".

Tunnel Emissions measured by the DustTrak were indistinguishable between the Fuel Combustion Regime during regeneration and the ambient phase. This was not surprising because the DustTrak does not measure ultrafine PM (<0.1 μm) that dominated the Fuel Combustion Regime. The low response of the DustTrak to ultrafine PM has been well-documented (Kinsey et al., 2006; Maricq, 2013; Quiros et al., 2013) and this work illustrates how the instrument is useful but should be used with knowledge of its limitations.

3.1.2.2. SMPS and EEPS. During the ambient and first idle phases, the SMPS (5.4–198 nm) and EEPS (C_1, 5.6–560 nm) measurements agreed within a factor of two and remained nearly constant, but five to ten times lower than the DustTrak rates. However at the peak concentration reported during the Soot Combustion Regime, Tunnel Emissions peaked at the same rate (~35 g PM/h) although the EEPS measures over a larger size range (5.6–560 nm) than the SMPS (5.5–198 nm). The emission of PM between 198 and 560 nm may have been negligible. Alternatively, particle concentrations measured by the two instruments may have differed by measurement principle.

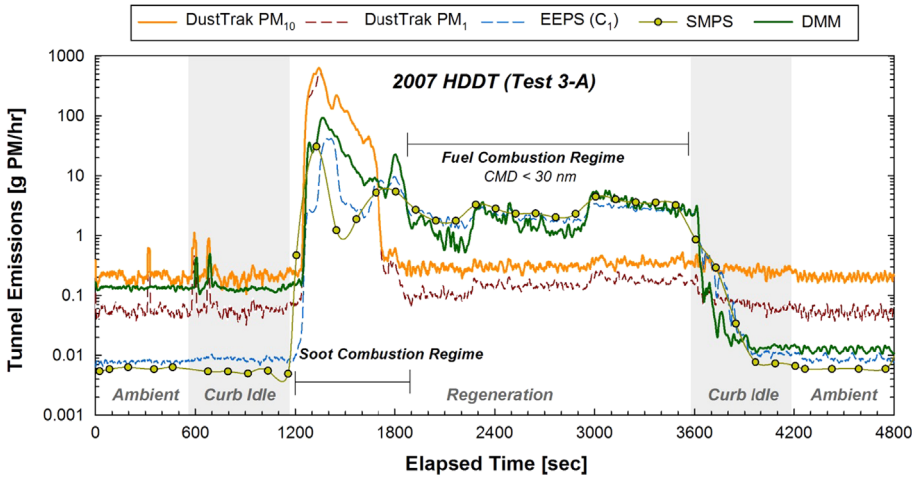

Fig. 3. Tunnel Emissions over all sequence phases measured by EEPS (C_1), SMPS, DMM, and DustTrak during test 3-A, an Initial Regeneration of the 2007 HDDT.

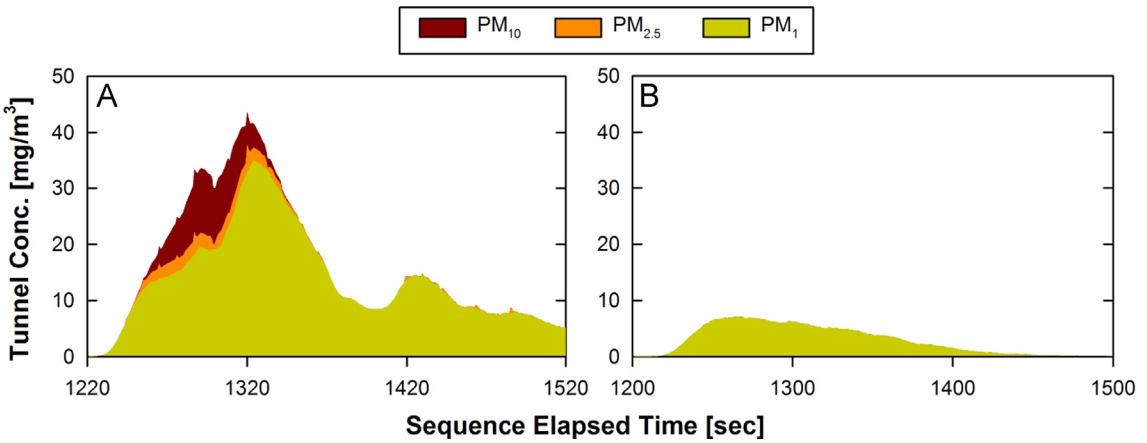

Fig. 4. PM_1, $PM_{2.5}$, and PM_{10} concentrations simultaneously measured by the DustTrak during two Initial Regenerations of the 2007 HDDT: (A) test 3-A and (B) test 2-A.

Relative to each other during the Fuel Combustion Regime, both instruments reported parallel shifts at 1800, 2300, and 3000 s. The explanation for these observed fluctuations is unclear because fuel injection rates remained constant at 0.3 L/min over this period. After the regeneration shut off during test 3-A, Tunnel Emissions reported by the EEPS and SMPS gradually declined during the idle phase to those observed during the initial ambient phase. According to Insite OBD data, engine exhaust and aftertreatment temperatures dissipated over five minutes (300 s) due to thermal inertia, consistent with emissions data. During both regimes, SMPS measurements confer adequate sensitivity to capture any transient shift in concentration reported by EEPS measurements.

3.1.2.3. DMM. The DMM (0.01–1.3 μm) supplemented the suite of PM instruments during test 3-A (Fig. 3) only. During the Soot Combustion Regime, the DMM measured a peak Tunnel Emissions rate of 80 g PM/h, approximately six times lower than DustTrak PM_1, but two times larger than the EEPS and SMPS. Given that the DMM and DustTrak PM_1 upper cutoff sizes are closely matched, observed emissions differences indicate the density calculated and applied by the DMM was lower than the density inherent in the factory ATD-based DustTrak calibration.

During the Fuel Combustion Regime, the DMM also detected the definitive shifts in Tunnel Emissions at three time points reported by EEPS and SMPS measurements (at 1800, 2300, and 3000 s). The DMM also reported the Tunnel Emissions decreased an order of magnitude from 0.15 to 0.015 g PM/h between the ambient phases before and after the regeneration. The corresponding concentrations of suspended mass were 10 and 1 $\mu g/m^3$, respectively, the latter of which is the lower detection limit of the DMM. The impacts of these fluctuations were trivial for measuring regeneration emissions at concentrations three orders of magnitude larger. Our data do not support use of the DMM for low PM mass measurement, a loose term defined here as any concentration below 10 $\mu g/m^3$.

3.1.3. Average Regeneration Emissions of the 2007 HDDT

3.1.3.1. Initial Regenerations. Figure 5 presents regeneration-average emissions from all tests conducted on the 2007 MY. Initial regeneration events shown in Fig. 5(a) all began in the Soot Combustion Regime where the magnitude of emissions positively correlated with the severity of DPF loading. For this comparison, EEPS (C_1C_2) data are presented where EEPS measurements were corrected to an SMPS equivalent. After grouping data by test sequence phase, the ratio of the lognormal fits of EEPS and SMPS measurements was computed and applied to EEPS (C_1) data to calculate the real-time SMPS equivalent. Using this approach, the size distribution is reported in terms of SMPS measurements but from higher time-resolved EEPS measurements. A comparison among EEPS, EEPS (C_1), and EEPS (C_1C_2) is presented in Section 3.3, and more details about the derivation of lognormal fit equations and corresponding correction equations are contained in Section 2 of Supporting information.

Test 1-A was initiated on an "Above Normal – Severe" DPF loading and resulted in the greatest Tunnel Emissions measured by all instruments: ~157 g PM_{10}/h by the DustTrak, 35 g PM/h by the gravimetric filter, and 31 g PM/h by the EEPS. The average rate over the regeneration for test 1-A was disproportionately larger than for the other tests because test 1-A test was aborted immediately following the high mass emissions of the regeneration Soot Combustion Regime and therefore did not include lower mass emission rates that would have been observed in the Fuel Combustion Regime.

Test 2-A was initiated when the dashboard indicator light was solid but not flashing indicating an "Above Normal – Least Severe" DPF loading. As shown in Fig. 4(b), the DustTrak classified all PM emissions as < 1 μm. The EEPS reported a negligible contribution of mass emissions for the 198–560-nm fraction, and because it is unlikely a second mass mode was present between 560 nm and 1 μm, these EEPS data show that virtually all Tunnel Emissions during test 2-A were from particles < 198 nm.

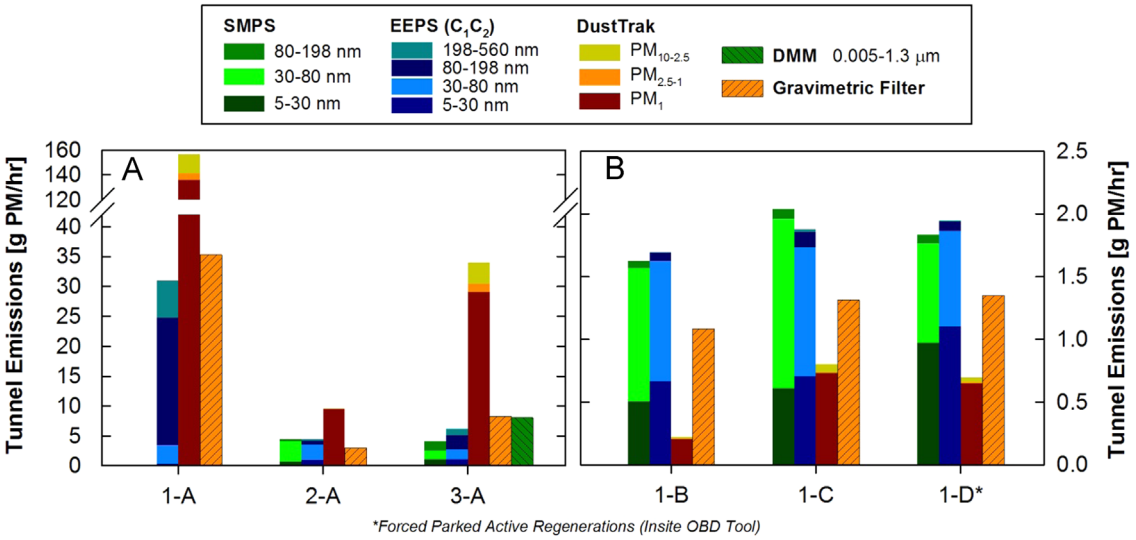

Fig. 5. 2007 HDDT: average Tunnel Emissions measured SMPS, EEPS (C_1C_2), DustTrak, DMM, and gravimetric filters during (A) Initial Regenerations and (B) Subsequent Regenerations.

Test 3-A was initiated on a second "Above Normal – Severe" DPF loading where resulting average Tunnel Emissions rates of 34, 8.4, 8.1, 6.3, and 4.0 g PM/h for the DustTrak PM_{10}, gravimetric filter, DMM, EEPS (C_1C_2), and SMPS, respectively. Similar to Test 1-A, the DustTrak size fractions indicated direct emission of PM in the fine and coarse fractions. Tunnel emissions measured by the EEPS and SMPS were typically within 10%, except the EEPS reported 50% more mass between 80 and 195 nm than the SMPS, and due to its larger size range reported about one-fifth of its total measured mass between 198 and 560 nm. The DMM reported 8.1 g PM/h suggesting about one-quarter of the mass emissions (1.8 g PM/h) were larger than 560 nm but below the upper measurement limit at 1.3 μm.

3.1.3.2. Subsequent Regenerations. Figure 5(b) shows the Subsequent Regenerations, where there were lower Tunnel Emissions, less intra-test variability among instruments, and less inter-test variability among regenerations. Tests 1-B and 1-C were initiated by a dashboard button, but test 1-D was a "forced" active parked regeneration that required using the Insite OBD tool. The emissions during this regeneration represent the result fuel injection into an already completely regenerated DPF. Tunnel Emissions rates measured by SMPS and EEPS (1.5–2 g PM/h) were about 50% more than the gravimetric filter rate (1.0–1.5 g PM/h) for Subsequent Regenerations 1-B, 1-C, and 1-D. For Subsequent Regenerations, the DustTrak *underestimated* Tunnel Emissions due to its limited response to ultrafine PM.

Based on DustTrak PM_{10} measurements of Tunnel Emissions during the ambient phases, dilution air contributions were 29%, 67%, and 96% of uncorrected particle mass flow through the tunnel for tests 1-B through 1-D, respectively. The successive increase in ambient contributions demonstrates two critical points. First, that although the Fuel Combustion Regime by our definition is where CMD remains <30 nm, direct emissions of larger PM fractions were still observed. And second, that dilution air accounted for a dominant fraction of total mass flux through the tunnel. Therefore the ambient-dilution wind tunnel is a good tool for evaluating the effect of diluting exhaust emissions into ambient air, and underscores the importance of monitoring dilution air in engine exhaust testing studies.

3.2. 2010 MY HDDT

3.2.1. Real-time PM mass emissions

Figure 6 presents a contour plot of the EEPS (C_1) distribution during test 4-A, an Initial Regeneration from the 2010 MY. PM mass emissions increased above ambient baseline levels ~300 s after initiating regeneration (1500 s), which was longer than the ~100 s observed for the 2007 MY (1300 s). For the 2010 MY, the Soot Combustion Regime was less pronounced in concentration and duration, and had lower peak CMD (40–50 nm) than the 2007 MY (100–200 nm). Furthermore, the Soot Combustion Regime for the 2010 MY only accounted for 5% of the total PM mass emissions, whereas 95% were emitted during the Fuel Combustion Regime. The Fuel Combustion Regime was similar between the two MYs where particle number concentrations exceeded 10^7 particles/cm^3, the CMD remained below 30 nm, and the observed nucleation possibly from the release of stored sulfur could be repressed for extended periods of time (Herner et al., 2011). Regardless of composition, particles 30 nm or smaller dominated, on a mass basis, the PM emissions during parked active regeneration of the 2010 MY truck.

Figure 7 presents Tunnel Emissions from the same Initial Regeneration shown in Fig. 6 as measured by EEPS (C_1, 5.6–560 nm), SMPS (5.4–198 nm), and DustTrak PM_{10} and PM_1. Tunnel Emissions measured by all instruments (g PM/h)

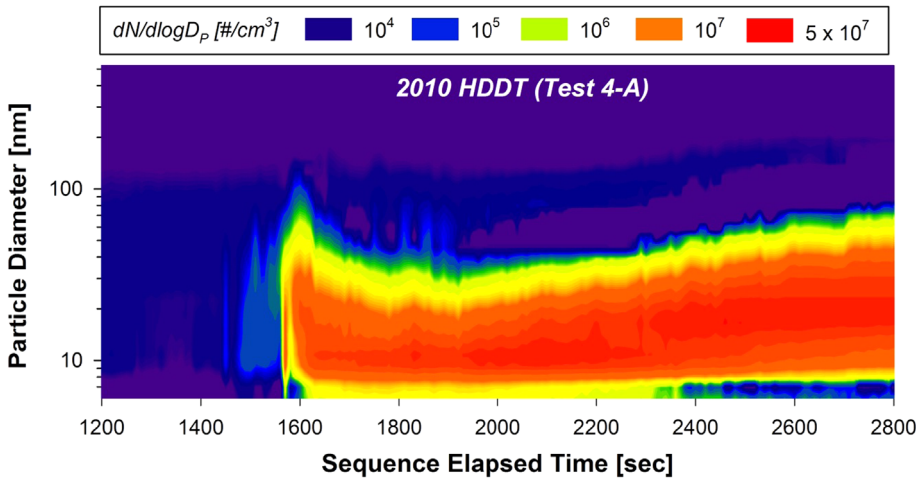

Fig. 6. Contour plot showing EEPS (C_1) number-based size distributions during test 4-A, an Initial Regeneration of the 2010 HDDT.

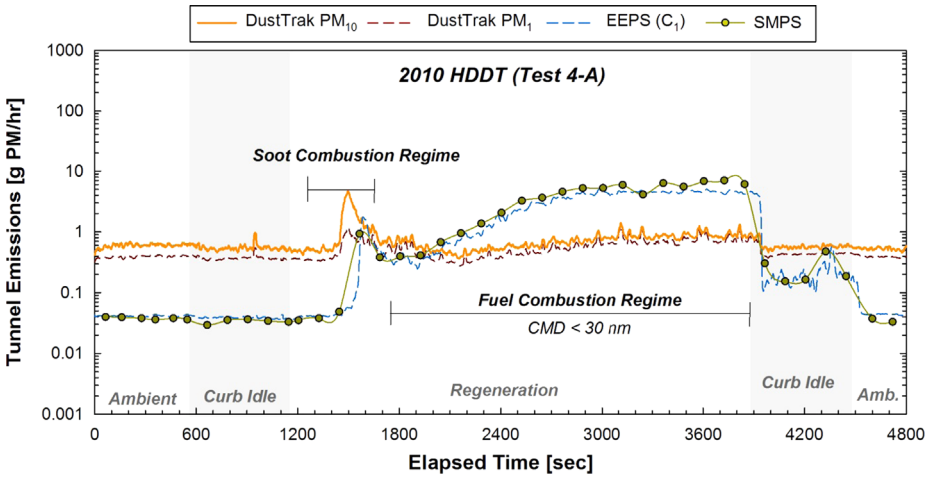

Fig. 7. Tunnel Emissions over all sequence phases measured by EEPS (C_1), SMPS, and DustTrak during test 4-A, an Initial Regeneration of the 2010 HDDT.

remained essentially unchanged from ambient to idle upon engine cold-start (600 s). The response of the instruments during regeneration described below.

3.2.1.1. DustTrak DRX. During the Soot Combustion Regime, the DustTrak PM_{10} Tunnel Emissions increased ten-fold relative to the ambient phase. The DustTrak emissions rate during test 4-A is shown on a linear scale in Fig. 8(a) where 60% of PM was larger than one micron. Although a definitive increase of directly-emitted coarse PM was observed for during test 4-A of the 2010 MY, the measured tunnel concentration (0.25 mg/m^3, dilution ratio ≈ 36) was over one hundred times lower than the 2007 MY (40 mg/m^3, dilution ratio ≈ 31). There were no visible emissions leaving the tunnel during regeneration of the 2010 HDDT. Figure 8(b) shows the DustTrak did not measure PM from any size fraction during test 4-B, a forced parked active Subsequent Regeneration emitting strictly within the Fuel Combustion Regime.

3.2.1.2. EEPS and SMPS. Figure 7 shows Tunnel Emissions measured by the SMPS and EEPS (C_1) tracked each other throughout test 4-A. During the Soot Combustion Regime, SMPS and EEPS (C_1) reported ~1.0 and ~1.8 g PM/h respectively near 1600 s. These data suggest two distinct mass peaks were emitted: initially a coarse-fraction peak near 1500 s measured by the DustTrak followed by an ultrafine-fraction peak measured by EEPS and SMPS near 1600 s. Use of a standalone electrical mobility instrument (EEPS or SMPS) or a photometric instrument (DustTrak) would therefore have resulted in overlooking one of the two peaks observed within the Soot Combustion Regime. Tunnel Emissions during the Fuel Combustion Regime increased asymptotically from 0.5 g PM/h with a CMD of ~12 nm to ~6 PM/h with a CMD of ~24 nm. The increasing trend was also observed for test 5-A (not shown), and contrasts with the CMD remaining constant with time in the Fuel Combustion Regime of the 2007 MY.

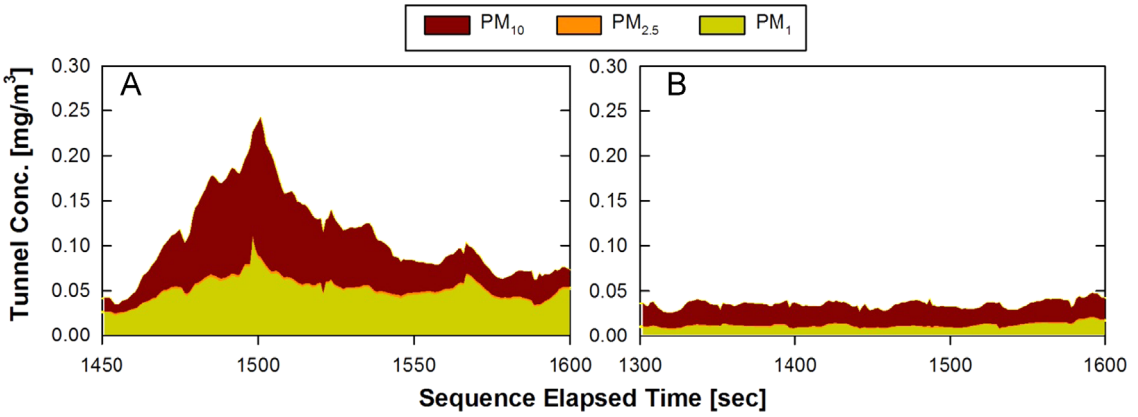

Fig. 8. PM_1, $PM_{2.5}$, and PM_{10} concentrations simultaneously measured by the DustTrak during two regenerations of the 2010 HDDT: (A) test 4-A and (B) test 4-B.

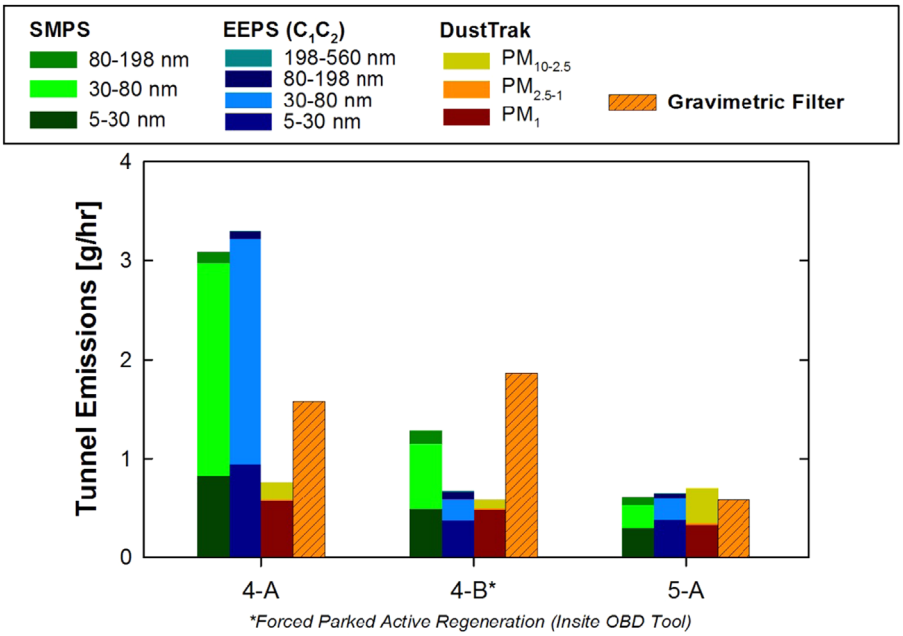

Fig. 9. 2010 HDDT: average Tunnel Emissions measured SMPS, EEPS (C_1C_2), DustTrak, and gravimetric filters during all regenerations.

3.2.2. *Average Regeneration Emissions of the 2010 HDDT*

Figure 9 shows average regeneration emissions for test 4-A: ~0.58 g $PM_{2.5}$/h and 0.76 g PM_{10}/h by the DustTrak, 1.6 g PM/h by the gravimetric filter, 3.1 g PM/h by SMPS, and 3.3 g PM/h by EEPS (C_1C_2). The contribution of ambient PM to Total Emissions was $<1\%$ for EEPS and SMPS measurements, but as large as 73% for DustTrak PM_{10}. Therefore EEPS or SMPS measurements have negligible impact from ambient contributions but are highly responsive to measuring DPF regeneration emissions.

Test 4-B was a Subsequent *forced active* Regeneration on a completely regenerated DPF, and similar to every other Subsequent Regeneration, the Fuel Combustion Regime dominated. Tunnel Emissions measured by SMPS were about 50% greater than EEPS (C_1C_2) emissions that primarily arose from a discrepancy in measuring the 80–198 nm fraction. Ambient contributions to PM_{10} was 83%, indicating only 17% of emissions within its measurement range were from the HDDT.

Test 5-A also initiated on an "Above Normal – Least Severe" DPF loading, but the regeneration was terminated by the engine control module earlier than during test 4-A (after 1000 s of regeneration, see Table 2). The Tunnel Emissions measured by SMPS, EEPS (C_1C_2), DustTrak PM_{10}, and gravimetric filter were 0.6–0.7 g PM/h. The values of EEPS and SMPS size fractions 5–30, 30–80, and 80–198 nm measured were within 10%, and the EEPS reported $<1\%$ of total Tunnel Emissions were from the 198–560-nm fraction. Based on DustTrak PM_{10} measurements, 66% of Tunnel Emissions were due

to ambient dilution air. During this test, all methods showed agreement at average emissions between 0.6 and 0.7 g PM/h, although filter values were expected to be the sum of ultrafine mass detected by the EEPS/SMPS and larger ambient PM detected by the DustTrak.

3.3. Measuring real-time PM mass

3.3.1. EEPS and SMPS

Figures 3 and 7 show Tunnel Emissions measured by the EEPS (C_1) were often lower than measured by the SMPS, especially during the Fuel Combustion Regime. Mass-based size distributions for test 3-A measured by the SMPS, EEPS (C_1), and DMM are plotted in Fig. 10. Peak concentration at the mass median diameter (MMD) measured by the SMPS was 33% and 87% larger than measured by the EEPS for Fuel and Soot Combustion Regimes, respectively. Despite SMPS and EEPS agreement when measuring a laboratory-generated calibration aerosol, the impact of aerosol characteristics on measurement is substantial and has been previously discussed (Asbach et al., 2009; Johnson et al., 2004; Oh et al., 2004). Although a detailed discussion of the measurement principles is beyond the scope of this study, the bipolar charging and CPC detection of the SMPS is regarded as more accurate than the unipolar corona charging and electrometer detection of the EEPS. Therefore the relationship between SMPS and EEPS measurements was used to develop a novel post-hoc correction for EEPS data (Supporting information, Section 2).

Figure 11 presents the gravimetric-normalized ratios of Tunnel Emissions for uncorrected EEPS (reported), zero-corrected EEPS (C_1), and zero and the post-hoc, or SMPS-corrected, EEPS (C_1C_2) measured by each instrument divided by the respective gravimetric filter value. Viewing data as a ratio facilitates an easier comparison among instruments relative to a baseline reference. The EEPS (C_1) correction resulted in an increased emissions rate by 0.3 to 4.7% depending on the test. Therefore even if zeroes are reported in raw EEPS data, the majority of PM on a mass basis would still be reported. The EEPS (C_1C_2) correction induced more dramatic impacts on reported emissions; corrections changed measurements from 64% lower (test 1-D) to 140% higher (test 2-A) than the EEPS (C_1) Tunnel Emission rate. Better agreement was reached between EEPS and SMPS Tunnel Emissions after applying the EEPS (C_1C_2) except for test 4-B where a larger discrepancy was observed.

Initial Regenerations resulted in gravimetric-normalized EEPS (C_1C_2) ratios ranging from 0.75 to 1.48 for the 2007 MY, and 1.14 to 2.08 for the 2010 MY. Subsequent Regenerations resulted ratios ranging 1.43–1.56 for the 2007 MY and 0.37 for the 2010 MY. Because filters collect particles of all sizes, these ratios are *underestimates* of the real differences between the applied effective density between 5.6 and 560 nm because the EEPS does not measure larger size fractions in the Tunnel Emissions. Selecting tests based on a smaller-size DustTrak distribution, the most reasonable gravimetric-normalized EEPS (C_1C_2) emissions ratios for the 5.6–560-nm range were approximately 1.5 for the 2007 HDDT, and 2.1 for the 2010 HDDT.

In summary, unless the manufacturer, TSI, provides an inversion matrix updated to address the observed discrepancies between EEPS and SMPS measurements shown in Figs. 3, 7, and 11, our data support applying a post-hoc correction procedure for EEPS data. In addition, the accuracy of calculating PM mass from real-time SMPS or EEPS measurements of electrical mobility would most certainly be improved by refining the effective density function for an array of discrete new types of new technology PM.

3.3.2. DustTrak DRX

The merit and faults of the DustTrak DRX for DPF regeneration studies are clear: it qualitatively provides size distribution over a large size and concentration, but it fails to measure ultrafine PM and is factory calibrated to ATD that does not

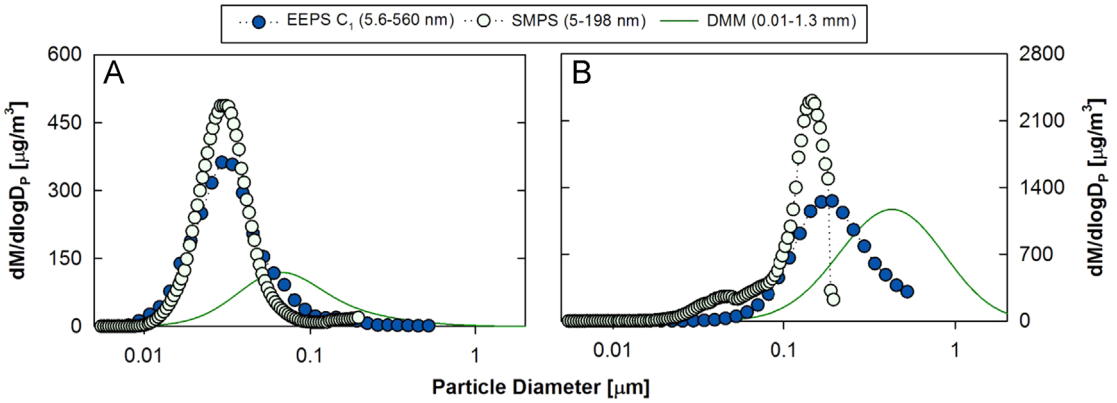

Fig. 10. Mass-based particle size distributions during test 3-A measured by the EEPS, SMPS, and DMM during the (A) Fuel Combustion Regime and (B) Soot Combustion Regime.

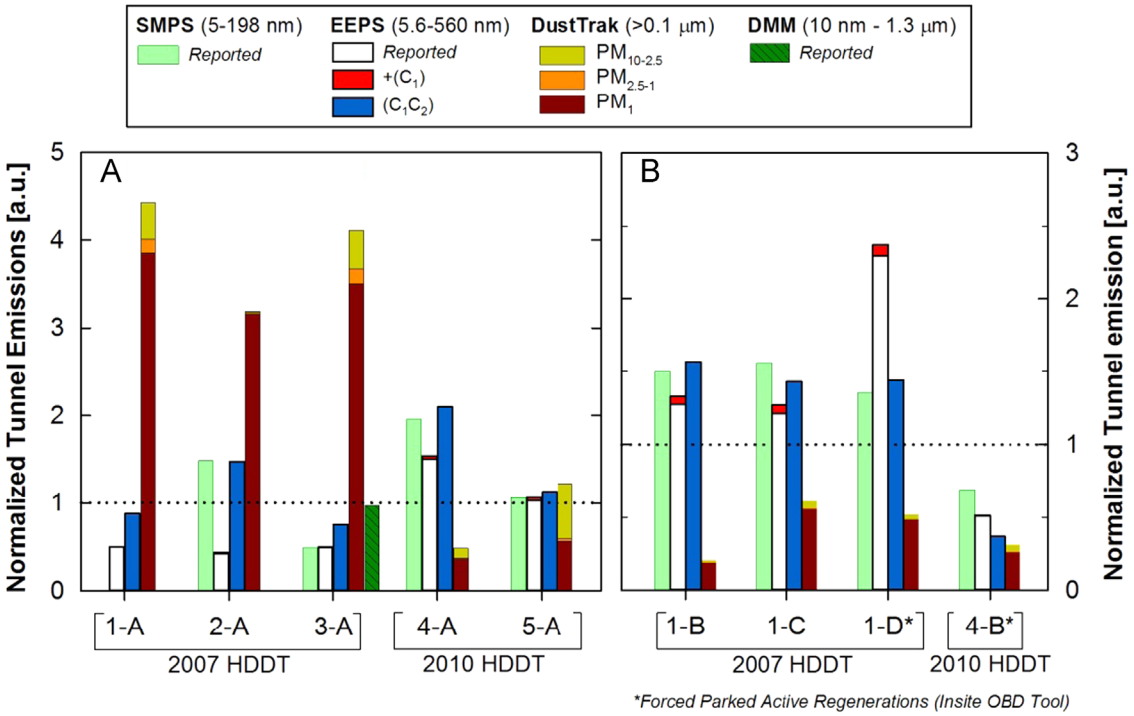

Fig. 11. Tunnel Emissions normalized to gravimetric measurements for regenerations of the 2007 and 2010 HDDT during (a) Initial Regenerations and (b) Subsequent Regenerations.

physical nor chemically represent vehicle emissions. To improve its accuracy, Appendix B of the DustTrak DRX Operation and Service Manual specifies to collect PM onto an on-board filter using an inlet impactor for derivation the photometric calibration factor for $PM_{2.5}$. Any calibration to a polydisperse aerosol with ultrafine PM will bias the calibration factor, however the bias is proportionally larger when measuring smaller size fractions. In this study, PM_{Total} was equivalent to PM_{10}, which resulted in an average gravimetric filter reference ratio of 3.91 for the 2007 MY. We recommend future studies to divide DustTrak reported values for all size fractions ($PM_{2.5}$, etc.) by 3.9 when measuring DPF regeneration that includes both a Soot and Fuel Combustion Regime.

3.3.3. DMM

The average mass-based distributions from test 3-A for the DMM are also shown for the Soot and Fuel Combustion Regimes in Fig. 10(a) and (b). Because the DMM reports mass directly, the average distributions were derived from a reported MMD and geometric standard deviation (GSD) reported at each one-second interval. DMM distributions were skewed-right with lower peak concentrations than EEPS and SMPS distributions. Figure 10(a) shows MMD for the DMM was ~60 nm during the Fuel Combustion Regime where a constant 1-g/cm^3 density was likely applied all particle sizes. Figure 10(b) shows MMD for the DMM was ~600 nm during the Soot Combustion Regime, still a much larger and broader distribution than obtained from the EEPS and SMPS. During the Soot Combustion Regime, the instrument should have calculated and applied an effective density function based on the relationship of mobility and aerodynamic distributions and soot decay function described by Virtanen et al. (2002). The MMD of the distributions between the DMM, SMPS, and EEPS should have agreed better because the density functions applied are functionally similar: the Virtanen et al. (2002) function applied by the DMM and the Maricq & Xu (2004) function shown in Eq. (2) and applied to EEPS/SMPS distributions. An evaluation of the density measurement approach employed by the DMM shows the average density is typically reported within 15% (Rostedt et al., 2009), although the discrepancies shown in Fig. 10 appear to be more of an error in measuring size distribution.

Figure 11 shows the Tunnel Emissions rate measured by the DMM for test 3-A agreed within five percent of the gravimetric reference using an undisclosed combination of reasonable algorithms to estimate particle density. The ostensible good agreement may be the result of the DMM having a relatively wide measurement range (0.01–1.3 μm) and high time resolution (1 Hz). However, rigorous testing would be required to demonstrate robust performance under a wide range of vehicle emissions. Furthermore, considering the discrepancy between the DMM size distribution and the EEPS or SMPS size distribution, the DMM should be tested alongside additional real-time instruments before used as standalone method for real-time mass measurement.

3.4. Discussion

This study measured ambient-diluted PM mass during parked active diesel particulate filter (DPF) regeneration of a 2007 and 2010 model year (MY) heavy-duty diesel trucks (HDDTs) using a TSI DustTrak DRX, TSI EEPS 3090, TSI SMPS 3936L88, DMM 230-A, and filters by gravimetric analysis. The strengths of each instrumental method are discussed; the principle limitation to measuring PM mass using the selected real-time methods is applying an appropriate particle density function. Gravimetric measurements indicated emissions from the 2007 MY were approximately an order of magnitude higher than the 2010 MY for Initial Regeneration events following equivalent treatments of on-road driving. The ten-fold reduction in PM mass emissions was largely due to a less dominant Soot Combustion Regime, which decreased from 75% to 5% of total regeneration emissions of the 2007 and 2010 MY, respectively. DustTrak emissions were divided by a factor of 3.9 to measure the proportion of the Soot Combustion Regime and SMPS measurements were used to measure the Fuel Combustion Regime. Applying this approach for test 3-A resulted in a mass apportionment of the two regimes to within five percent of those reported by the DMM.

Today in California, PM emissions during parked active regeneration represent an important category of PM emissions, even for on-road heavy-duty engines meeting the 2007 emissions standard (0.01 g PM/bhp-h). The comparability between PM emissions from parked active DPF regeneration versus other approaches for DPF regeneration is not entirely clear. In some cases, DPF regeneration may be initiated during on-road operation, either actively or passively. This study shows a sharp reduction trend in PM emissions during a discrete parked active DPF regeneration between the 2007 and 2010 MY. However, many factors influence engine-out PM emissions entering the DPF, the management of accumulated soot on inner surfaces, and total PM emissions over longer periods including non-regeneration periods.

The ambient-dilution wind tunnel used in this study is a useful tool for evaluating the controlled real-world dilution of exhaust gases. Particle number, count median diameter, and geometric standard deviation were not impacted by the incidental ranges of dilution air temperature, relative humidity, and ambient particulate characteristics. However, the observed count median particle diameter between 15 and 25 nm during the Fuel Combustion Regime was larger than 10 nm as reported by Herner et al. (2011) during DPF active regeneration where useful work was being produced by the engine and measurements were conducted using filtered laboratory air. On a mass basis, the contribution of ambient dilution air to tunnel mass flux (Tunnel Emissions) was substantial, sometimes exceeded the contribution from exhaust emissions. Therefore, dilution air should be always monitored under the present experimental setup. Future work could evaluate the interaction between ambient dilution air characteristics and regeneration emissions under higher dilution ratios, residence times, or newer HDDT models.

Acknowledgments

This work was funded by the California Air Resources Board (CARB) Research Division Contract #11-329. The authors thank Don Chernich and his staff in the Mobile Source Operations Division for their support during testing, including Mark Burnitzki, Robert Ianni, Roelof Riemersma, Wayne Sobieralski, and Tully Flower. The authors also thank Michael Werst and his staff in the Monitoring and Laboratory Division for their filter analysis work. The statements and opinions expressed in this paper are solely the authors' and do not represent the official position of California Air Resources Board (CARB). The mention of trade names, products, and organizations does not constitute endorsement or recommendation for use. CARB is a department of the California Environmental Protection Agency. CARB's mission is to promote and protect public health, welfare, and ecological resources through effective reduction of air pollutants while recognizing and considering effects on the economy. CARB oversees all air pollution control efforts in California to attain and maintain health-based air quality standards.

Appendix A. Supporting information

Supplementary data associated with this article can be found in the online version at http://dx.doi.org/10.1016/j.jaerosci.2014.03.002.

References

Asbach, C., Kaminski, H., Fissan, H., Monz, C., Dahmann, D., Mülhopt, S., Paur, H., Kiesling, H., Herrmann, F., Voetz, M., & Kuhlbusch, T.J. (2009). Comparison of four mobility particle sizers with different time resolution for stationary exposure measurements. *Journal of Nanoparticle Research*, *11*, 1593–1609.

Barone, T.L., Storey, J.M.E., & Domingo, N. (2010). An analysis of field-aged diesel particulate filter performance: particle emissions before, during, and after regeneration. *Journal of the Air and Waste Management Association*, *60*, 968–976.

Burtscher, H. (2005). Physical characterization of particulate emissions from diesel engines: a review. *Journal of Aerosol Science*, *36*, 896–932.

Bushkuhl, J., Silvis, W., Maricq, M.M., & Szente, J. (2013). A new approach for very low particulate mass emissions measurement. SAE 2013-01-1557.

Cauda, E., Fino, D., Saracco, G., & Specchia, V. (2007). Secondary nanoparticle emissions during diesel particulate trap regeneration. *Topics in Catalysis 42–43*, 253–257.

Dwyer, H. (2013). *Measurement of emissions from both active and parked regenerations of a diesel particulate fitler from heavy duty trucks*. California Air Resources Board: (Final report, agreement number 11-329).

EPA, U.S. (2002). Health assessment document for diesel engine exhaust. United States Environmental Protection Agency. EPA/600/8-90/057F.
Grose, M., Sakurai, H., Savstrom, J., Stolzenburg, M.R., Watts, W.F., Morgan, C.G., Murray, I.P., Twigg, M.V., Kittelson, D.B., & McMurry, P.H. (2006). Chemical and physical properties of ultrafine diesel exhaust particles sampled downstream of a catalytic trap. *Environmental Science and Technology*, *40*, 5502–5507.
Harrison, R.M., Shi, J.P., Xi, S., Khan, A., Mark, D., Kinnersley, R., & Yin, J. (2000). Measurement of number, mass and size distribution of particles in the atmosphere. *Philosophical Transactions of the Royal Society of London. Series A: Mathematical, Physical and Engineering Sciences*, *358*, 2567–2580.
Herner, J.D., Hu, S., Robertson, W.H., Huai, T., Chang, M.C.O., Rieger, P., & Ayala, A. (2011). Effect of advanced aftertreatment for PM and NO_x reduction on heavy-duty diesel engine ultrafine particle emissions. *Environmental Science and Technology*, *45*, 2413–2419.
Hinds, W.C. (1999). *Aerosol Technology, Properties Behavior and Measurement of Airborne Particles* 2nd ed). .
Johnson, T., Caldow, R., Pocher, A., Mirme, A., & Kittelson, D. (2004). A new electrical mobility particle sizer spectrometer for engine exhaust particle measurements. SAE 2004-01-1341.
Khalek, I.A. (2005). *2007 Diesel particulate measurement research*. Coordinating Research Council: (Final report, project E-66-Phase 1).
Khalek, I.A., Bougher, T.L., Merritt, P.M., & Zielinska, B. (2011). Regulated and unregulated emissions from highway heavy-duty diesel engines complying with U.S. Environmental Protection Agency 2007 Emissions Standards. *Journal of the Air and Waste Management Association*, *61*, 427–442.
Khan, M.Y., Johnson, K.C., Durbin, T.D., Jung, H., Cocker, D.R., III, Bishnu, D., & Giannelli, R. (2012). Characterization of PM-PEMS for in-use measurements conducted during validation testing for the PM-PEMS measurement allowance program. *Atmospheric Environment*, *55*, 311–318.
Kinsey, J.S., Mitchell, W.A., Squier, W.C., Linna, K., King, F.G., Logan, R., Dong, Y., Thompson, G.J., & Clark, N.N. (2006). Evaluation of methods for the determination of diesel-generated fine particulate matter: physical characterization results. *Journal of Aerosol Science*, *37*, 63–87.
Kittelson, D.B., Watts, W.F., Johnson, J.P., Rowntree, C., Payne, M., Goodier, S., Warrens, C., Preston, H., Zink, U., Ortiz, M., Goersmann, C., Twigg, M.V., Walker, A.P., & Caldow, R. (2006). On-road evaluation of two diesel exhaust aftertreatment devices. *Journal of Aerosol Science*, *37*, 1140–1151.
Lehmann, U., Niemelä, V., & Mohr, M. (2004). New method for time-resolved diesel engine exhaust particle mass measurement. *Environmental Science and Technology*, *38*, 5704–5711.
Liu, B.Y.H., Pui, D.Y.H., Rubow, K.L., & Szymanski, W.W. (1985). Electrostatic effects in aerosol sampling and filtration. *Annals of Occupational Hygiene*, *29*, 251–269.
Liu, Z.G., Vasys, V.N., Dettmann, M.E., Schauer, J.J., Kittelson, D.B., & Swanson, J. (2009). Comparison of strategies for the measurement of mass emissions from diesel engines emitting ultra-low levels of particulate matter. *Aerosol Science and Technology*, *43*, 1142–1152.
Lloyd, A.C., & Cackette, T.A. (2001). Diesel engines: environmental impact and control. *Journal of the Air and Waste Management Association*, *51*, 809–847.
Mamakos, A., Ntziachristos, L., & Samaras, Z. (2006). Evaluation of the Dekati mass monitor for the measurement of exhaust particle mass emissions. *Environmental Science and Technology*, *40*, 4739–4745.
Maricq, M.M. (2013). Monitoring motor vehicle PM emissions: an evaluation of three portable low-cost aerosol instruments. *Aerosol Science and Technology*, *47*, 564–573.
Maricq, M.M., & Xu, N. (2004). The effective density and fractal dimension of soot particles from premixed flames and motor vehicle exhaust. *Journal of Aerosol Science*, *35*, 1251–1274.
Maricq, M.M. (2007). Chemical characterization of particulate emissions from diesel engines: a review. *Journal of Aerosol Science*, *38*, 1079–1118.
May, A.A., Presto, A.A., Hennigan, C.J., Nguyen, N.T., Gordon, T.D., & Robinson, A.L. (2013). Gas-particle partitioning of primary organic aerosol emissions: (2) diesel vehicles. *Environmental Science and Technology*, *47*, 8288–8296.
Oh, H., Park, H., & Kim, S. (2004). Effects of particle shape on the unipolar diffusion charging of nonspherical particles. *Aerosol Science and Technology*, *38*, 1045–1053.
Quiros, D.C., Lee, E.S., Wang, R., & Zhu, Y. (2013). Ultrafine particle exposures while walking, cycling, and driving along an urban residential roadway. *Atmospheric Environment*, *73*, 185–194.
Rostedt, A., Marjamäki, M., & Keskinen, J. (2009). Modification of the ELPI to measure mean particle effective density in real-time. *Journal of Aerosol Science*, *40*, 823–831.
Russell, L.M., Flagan, R.C., & Seinfeld, J.H. (1995). Asymmetric instrument response resulting from mixing effects in accelerated DMA-CPC measurements. *Aerosol Science and Technology*, *23*, 491–509.
Timko, M.T., Yu, Z., Kroll, J., Jayne, J.T., Worsnop, D.R., Miake-Lye, R.C., Onasch, T.B., Liscinsky, D., Kirchstetter, T.W., Destaillats, H., Holder, A.L., Smith, J.D., & Wilson, K.R. (2009). Sampling artifacts from conductive silicone tubing. *Aerosol Science and Technology*, *43*, 855–865.
TSI (2011). Fast mobility sizers, FMPS 3091, EEPS 3090, standard operating procedure. In: Fast sizing workshop 2011. TSI.
Virtanen, A., Ristimäki, J., Marjamäki, M., Vaaraslahti, K., Keskinen, J., & Lappi, M. (2002). Effective density of diesel exhaust particles as a function of size. SAE 2002-01-0056.
Wang, J., Storey, J., Domingo, N., Huff, S., Thomas, J., & West, B. (2006). Studies of diesel engine particle emissions during transient operations using an engine exhaust particle sizer. *Aerosol Science and Technology*, *40*, 1002–1015.
Wang, S.C., & Flagan, R.C. (1990). Scanning electrical mobility spectrometer. *Aerosol Science and Technology*, *13*, 230–240.
Wang, X., Chancellor, G., Evenstad, J., Farnsworth, J.E., Hase, A., Olson, G.M., Sreenath, A., & Agarwal, J.K. (2009). A novel optical instrument for estimating size segregated aerosol mass concentration in real time. *Aerosol Science and Technology*, *43*, 939–950.
Yanosky, J.D., Williams, P.L., & MacIntosh, D.L. (2002). A comparison of two direct-reading aerosol monitors with the federal reference method for PM2.5 in indoor air. *Atmospheric Environment*, *36*, 107–113.
Zheng, Z., Johnson, K.C., Liu, Z., Durbin, T.D., Hu, S., Huai, T., Kittelson, D.B., & Jung, H.S. (2011). Investigation of solid particle number measurement: existence and nature of sub-23 nm particles under PMP methodology. *Journal of Aerosol Science*, *42*, 883–897.
Zhu, Y.F., Hinds, W.C., Kim, S., Shen, S., & Sioutas, C. (2002). Study of ultrafine particles near a major highway with heavy-duty diesel traffic. *Atmospheric Environment*, *36*, 4323–4335.